Int J Adv Manuf Technol (2017) 90:875–885
DOI 10.1007/s00170-016-9439-x

ORIGINAL ARTICLE

Springback prediction and compensation for the third generation of UHSS stamping based on a new kinematic hardening model and inertia relief approach

Zhenzhen Wang[1] · Qi Hu[1] · Jiawei Yan[1] · Jun Chen[1]

Received: 24 July 2016 / Accepted: 4 September 2016 / Published online: 14 September 2016

Abstract Ultrahigh-strength steel (UHSS), such as DP980, has been widely used in automotive structural components to further reduce the weight of the autobody and improve the crashworthiness performance. However, UHSS sheets demonstrate more obvious kinematic hardening, which results in severe springback. In the present work, the kinematic hardening of typical Quenching and Partitioning steel, QP980, which is the typical steel of third generation of UHSS, is tracked by using a nonsaturating kinematic (NSK) Swift model in order to simulate the loading process more accurately. For unloading process, inertia relief is adopted as a new control approach in springback calculation. The experiment results show that the NSK Swift model improves the springback prediction accuracy greatly compared with that predicted by isotropic hardening model, and the inertia relief is validated as an accurate and efficient springback calculation method. Moreover, springback compensation based on the NSK Swift model can reach acceptable tolerance as ±0.5 mm through the iterative compensation method in LS-Dyna.

Keywords Springback · Hardening model · Inertia relief · Ultrahigh-strength steel (UHSS)

1 Introduction

Lightweight manufacturing in automotive industry has definitely become a reliable trend for the sake of energy conservation and emission reduction; accordingly, the application of ultrahigh-strength steels (UHSS) and other lightweight alloys is growing steadily. As the third generation of UHSS, QP steels show great application potentials in automobile structural components for its high strength and good ductility. Its tensile strength can reach up to 1000–1500 MPa, which belongs to the highest level of steels, and the forming process can be achieved at room temperature [1]. The main microstructure of QP steel is the combination of martensite, polygonal ferrite, and a considerable amount of retained austenite (RA) [2]. Martensite transformation from RA induced by deformation, namely, transformation-induced plasticity (TRIP) effect, promotes the capability of work hardening and consequent plasticity [3].

However, UHSS shows more severe springback than traditional mild steel and conventional high-strength steels in sheet metal forming due to its higher flow stress. Springback is undesirable because it decreases components' dimensional accuracy and influences the following forming process negatively. Consequently, the accurate springback prediction, control, and compensation of UHSS stamping are essential to deserve special attentions.

During the past decades, many researchers studied the factors which influence the springback and improved the accuracy of springback prediction. The previous researches proved that finite element analysis (FEA) is a viable and effective tool for springback prediction, but it is much more sensitive to material model and to numerical tolerances [4]. The effects of material models, finite element type, time integration scheme and contact algorithms have been extensively investigated [5]. Material behavior modeling mainly refers to yield function and hardening model [6]. A suitable yield function is indispensable to predict the material behavior in the plane stress state. Hill's [7, 8] quadratic yield function (Hill'48) and Barlat's [9] three-parameter yield function (Barlat

✉ Jun Chen
jun_chen@sjtu.edu.cn

[1] Department of Plasticity Technology, Shanghai Jiao Tong University, Shanghai 200030, China

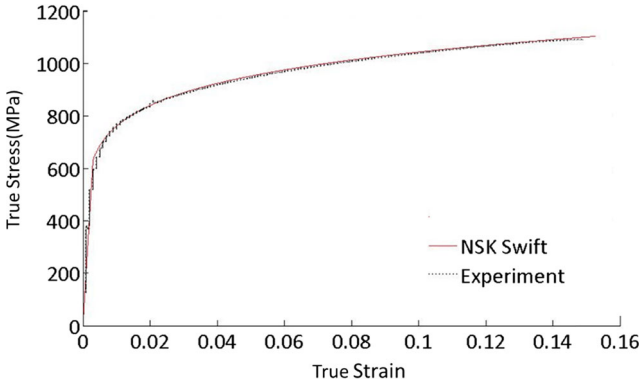

Fig. 1 Comparison of the NSK Swift model and the tensile test data (QP980)

YLD89) are being widely used to describe the yield surface anisotropy of UHSS stamping. Giving better descriptions of flow stress characteristics with the change of strain paths, such as Bauschinger effect, transient behavior, and permanent softening, nonlinear kinematic hardening (NLK) model is also considered as an efficient approach. Armstrong-Frederick [10] model is capable of predicting Bauschinger effect and transient behavior and is the basis of other modified models, such as Chaboche [11] hardening model and anisotropic nonlinear kinematic hardening (ANK) [12] hardening model. Another well-performed one in describing the cyclic hardening is Yoshida-Uemori [13] model, which introduces a backstress evolution equation and a nonisotropic hardening surface. Although Yoshida-Uemori model is able to describe cyclic deformation characteristics, four parameters and ten history variables need to be determined [14], which makes it rather difficult in convenient industrial applications. Nonsaturating kinematic (NSK) Swift model describing the nonsaturating cyclic hardening behavior is a newly proposed kinematic hardening model by Xiao et al. [15]. The NSK Swift model was well confirmed by predicting the springback and thickness of the UHSS metal (DP600 and DP965) in Benchmark 2 of numisheet 2005 by Chen et al. [16]. It is worth mentioning that the parameters of this model can be determined by only using the tensile test data, which means a practical significance in industrial application.

What is more, implicit springback analysis requires that rigid body modes be eliminated since dynamic inertia effects cannot be included in a static analysis. The inertia relief approach is a well-known method which is often combined with finite element method in analyzing unconstrained systems such as satellite in space, aircraft in flight, or automotive in motion [17]. Mark et al. [18] employed inertia relief to estimate impact load of a space frame structure composed of welded tubular elements. Baskar [19] evaluated door slam durability based on inertia relief method coupled with fatigue analysis. Anvari and Babak [20] compared the maximum stresses obtained from transient dynamics and inertia relief method for an unconstrained structure experiencing a dynamic force and concluded that the inertia relief approach is reliable and efficient. Singh [21] conducted the inertia relief analysis to obtain the cumulative damage and life of a refuse truck cab. Although inertia relief approach has been widely applied in the simulation of unconstrained aircraft, space vehicle, and automobile, the published work about the application of inertia relief in stamping springback prediction has rarely been found. Livermore Software Technology Corporation (LSTC) presented inertia relief as a new feature in LS-DYNA 971. This feature can be used in springback calculation to avoid artificial support constraints to remove model singularities.

Based on precise springback prediction, the methods to control springback of UHSS stamping are mainly classified into two catalogs: optimizing the forming parameters or springback compensation of tool surface. As the forming parameters optimization method, such as increasing the blank holder force, is not always feasible to reduce springback sufficiently, springback compensation is often used to achieve satisfactory result.

The most famous springback compensation method is displacement adjustment method (DA) [22, 23]. Weiher et al. [24] presented a new springback control strategy—

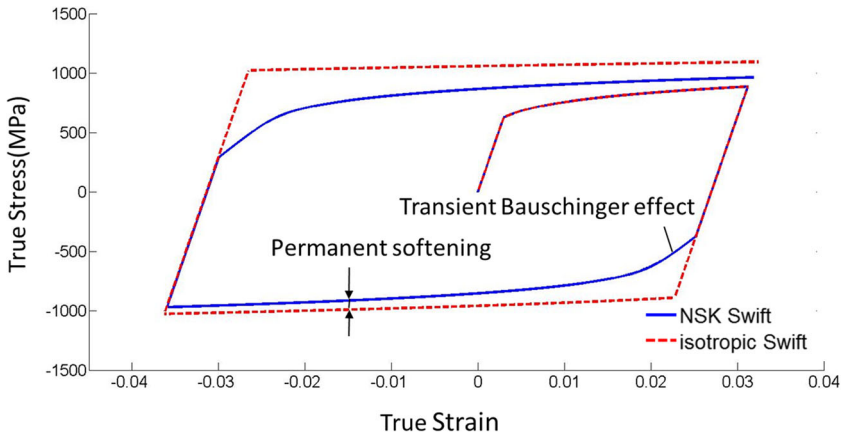

Fig. 2 Comparison of NSK Swift model with isotropic Swift model under cyclic loading (QP980)

Table 1 The material constants of the NSK Swift model from the tension data (QP980)

E (MPa)	μ	σ_0 (MPa)	C (MPa)	m	X_0 (MPa)	r		
						r_0	r_{45}	r_{90}
210,000.0	0.3	633.0	40,665.2	−6.7101	627.1	1.172	0.997	0.787

smooth displacement adjustment method (SDA)—based on DA method, to compensate the complete tool geometry including the addendum and the blank holder surfaces. Lingbeek et al. [25] also proved that the SDA method is effective in compensating springback in industrial productions. Yang and Ruan [26] proposed a new method which takes compensation direction into account based on DA method and concluded that the new method has a higher precision especially for complex panel with advanced high-strength sheet metals. Li et al. [27] developed a new springback compensation algorithm and system based on the advanced DA method for advanced high-strength steel (AHSS) parts and validated it with two engineering examples. Other innovative attempts about springback compensation have also been made. Fu and Mo [28] presented a new strategy for direct generation of die shapes from digitized points with springback compensation. Wang et al. [29] conducted springback compensation of automotive panel based on 3D scanning and reverse engineering for the formed part to reduce the number of die tryouts and tool development cycles. Wang et al. [30] introduced multiple-iteration springback compensation to improve the accuracy of springback compensation.

In order to exploit the application potential of QP steel, the NSK Swift model is applied to describe the hardening behavior of QP980 and the procedure of material constants determination with the tension test data for the NSK Swift model is illustrated thoroughly for further application, and comparative studies are made between numerical simulation result and experimental result. The inertia relief approach is also illustrated and further employed in springback calculation to examine the accuracy and efficiency. Springback compensation is further conducted based on the NSK Swift model and the iterative compensation method in LS-Dyna.

2 Theory and model

2.1 NSK Swift hardening model

Xiao and Chen et al. [15, 16, 31] developed the NSK Swift model in the energy-based framework which can also represent other different hardening laws. A short review of the NSK Swift model derivation is illustrated here.

Generally, the yield function is rewritten as below to introduce hardening behaviors [29].

$$f(\sigma_{\text{dev}}, X, R) := \overline{\sigma}\ (\sigma_{\text{dev}} - X) - (R + \overline{\sigma}_0) \le 0 \tag{1}$$

where σ_{dev} is the deviatoric stress, X is the back-stress, R is the isotropic strength, σ_0 is the initial yield stress, and $\overline{\sigma}$ is the equivalent stress function. With the yield function in Eq. (1), the isotropic Swift model is given as Eqs. (2) and (3).

$$R = k(\varepsilon_0 + \overline{\varepsilon}^p)^n - k_0 \tag{2}$$

$$k_0 = k(\varepsilon_0)^n \tag{3}$$

where k, n, and ε_0 are material parameters. According to the energy-based framework [15], the isotropic Swift model can be given in the unified rate form as

$$\dot{R} = K\dot{\overline{\varepsilon}}^p\,(1 - h_i) \tag{4}$$

where $\dot{\overline{\varepsilon}}^p$ is equivalent plastic strain rate and h_i is the control function for isotropic Swift law if it is incorporated into the framework [15],

$$h_i = 1 - \left(\frac{R}{k_0} + 1\right)^m \tag{5}$$

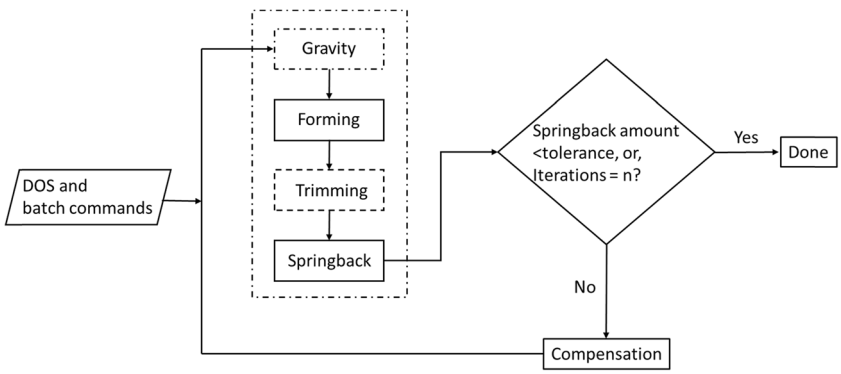

Fig. 3 Iterative springback compensation flowchart

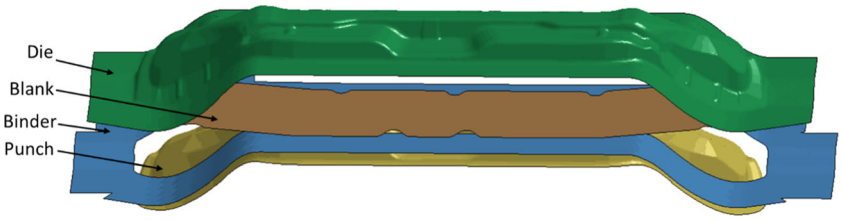

Fig. 4 The forming setup of the automotive covering part

where K, k_0, and m are material parameters.

The kinematic hardening models can also be expressed as below based on the energy-based framework.

$$\dot{X} = \frac{2}{3} C\dot{\varepsilon}^p - Ch_k^{'}\dot{\bar{\varepsilon}}^p n_X \tag{6}$$

where C is material constant related to the stored plastic energy in kinematic hardening and $n_X = X/\bar{X}$. By analogizing the isotropic control function, $h_k^{'}$ is control function for kinematic hardening as

$$h_k^{'} = h_k = 1 - \left(\frac{\bar{X}}{X_0} + 1\right)^m \tag{7}$$

where X_0 is stress-type material constant related to the initial value of X. Then, the NSK hardening is readily achieved as Eq. (7).

Moreover, Chen et al. [16] validated that in contrast to the isotropic Swift model, the NSK Swift model could well capture Bauschinger effect as well as the permanent offset of DP600 under cyclic loading and predict springback of an automobile underbody cross-member panel in Benchmark 2 of numisheet2005 more accurately with only using the tensile test data of the materials. For further application of the NSK Swift model, the procedure of material constant determination with the tension data is listed in detail as follows, taking QP980 for instance.

1. Calculate $\sigma_{0.2}$ on the engineering strain-stress curve and regard $\sigma_{0.2}$ as initial yield stress σ_0. For QP980, σ_0 = 633.0 MPa.
2. Modify the engineering stress-strain curve to the true stress-plastic strain curve and fit the curve with isotropic Swift model $s = K(\varepsilon_0 + \varepsilon)^n$ over the strain 0.14. For QP980, ε_0 = 0.002, K = 1404 MPa, n = 0.1297, k_0 = 627.1 MPa.
3. Obtain the material constants of the NSK Swift model from below equations.

$$C = nk^{\frac{1}{n}}(k_0)^m \tag{8}$$

$$m = 1 - 1/n \tag{9}$$

$$X_0 = k_0 \tag{10}$$

For QP980, C = 40,665.2 MPa, m = −6.7101, X_0 = 627.1 MPa.

As shown in Fig. 1, the NSK Swift model well describes the simple tension experiment data of QP980, which has validated the above transferring method of material constants from the isotropic Swift model to the NSK Swift model.

To further study the hardening behaviors of QP980 under cyclic loading, the comparison of isotropic hardening model and the NSK Swift model is made. The kinematic hardening behaviors, such as Bauschinger effect, transient behavior, and permanent softening, can be well captured by the NSK Swift model as shown in Fig. 2.

Moreover, the NSK Swift hardening model combined with Hill48 yield function is programmed in LS-Dyna through the user material interface for forming and springback simulation. The material constants of NSK Swift hardening model and Hill48 yield criterion are listed in Table 1.

2.2 Theory of inertia relief

Inertia relief method is used to analyze the structure by assuming that an equilibrium state exists between the external forces and the inertia forces due to rigid body accelerations produced by unconstrained motion [19]. During finite element analysis, inertia relief forces are calculated based on the rigid body modes and the mass matrix of the model [32]. If R represents the rigid body

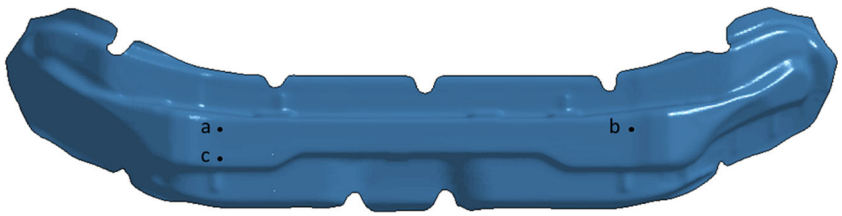

Fig. 5 Necessary constraints in springback calculation

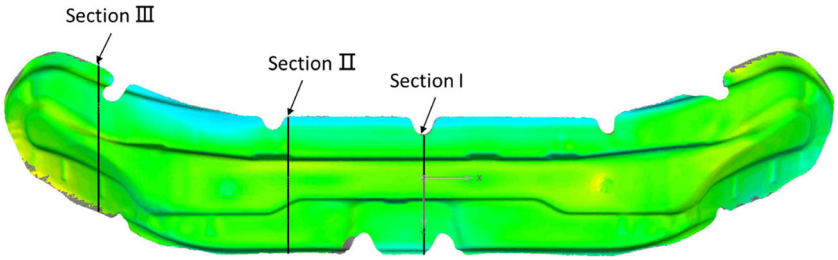

Fig. 6 The sections specified for springback comparison: **a** by CTN, **b** by IR

modes, M represents the mass matrix, F represents the load vector, and $\ddot{z}$ represents rigid body accelerations associated with the rigid body mode, the nodal force vector corresponding to the inertia relief load F^{ir} is calculated as follows:

$$F^{ir} = -MR\ddot{z} \tag{11}$$

In Eq. (11), $\ddot{z}$ is calculated by solving the following equation.

$$\left[R^T MR\right]\ddot{z} = R^T F \tag{12}$$

The corrected load vector is the original load vector minus the inertia relief load as follows:

$$F' = F - F^{ir} \tag{13}$$

Then, this corrected load vector without inertia relief loads is used in the static analysis. For this feature in LS-Dyna, eigenvalues have to be computed to find rigid body modes R, and then the model is constrained so that it does not move in the directions given by M^*R.

The implementation of the springback computation in LS-Dyna requires defining the THRESH value, which is the threshold for a rigid body mode. It is necessary to mention that users have to change the THRESH value based on real parts instead of using the default value. Using a too big value will constrain some other deformation modes while using a too small value will not effectively remove rigid body modes and cause divergence.

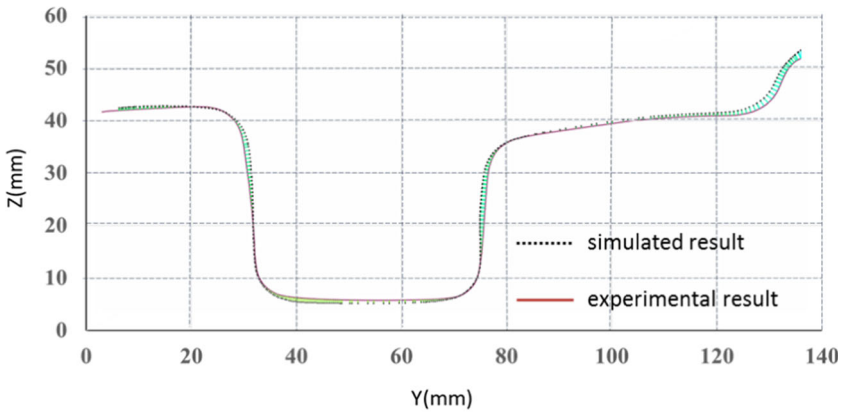

(a) By CTN

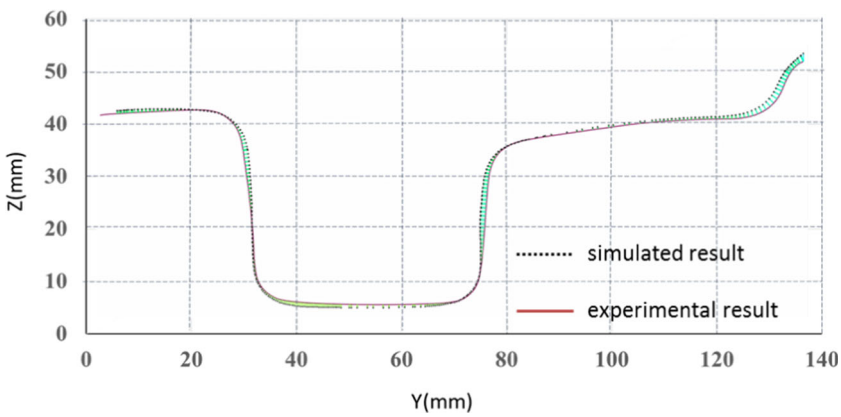

(b) By IR

Fig. 7 Comparison between the experiment data and the simulated results of springback profiles at section I: **a** by CTN, **b** by IR

2.3 Springback compensation

Springback compensation is the modification of the original tool surface geometry, reducing shape deviations between the final configuration of the part and the design intent. However, there are many challenges in springback compensation of stamping, such as undercut problem and difficulty in maintaining smooth addendum and binder. In LS-Dyna, the springback compensation code can automatically detect the undercut problem and seven extrapolation algorithms to get smooth surface have been proposed.

Moreover, compensation algorithm is a nonlinear iterative method and one iteration of compensation is usually not enough to reduce the part deviation to the acceptable tolerance. As shown in Fig. 3, LS-Dyna adopts iterative method and more iterations can be used until the final springback amount meets the allowable tolerance. With a few DOS commands and batch commands, this iterative loop can be completed automatically.

3 Springback prediction

3.1 Forming simulation setup

The selected case for study is the lower member-dash, an automotive structural part. The setup of the simulation model for forming process is shown in Fig. 4. As we all know, accurate prediction of forming stress distribution is essential to springback prediction. Therefore, more attentions should be paid on the accuracy of material constants and simulation parameters in forming stage. The material constants of QP980 are derived and validated in Sect. 2 and employed in the simulation. The initial shell element size is 6 mm, and the adaptive remeshing level is set as 4. The fully integrated shell formulation and seven integration points in the shell section are considered in forming and springback stages. The blank thickness is 2 mm, and the closing gap between the die and the punch is 2.2 mm. The binder force is set as 1000 kN following the actual experiment condition, and the virtual stamping velocity is defined as 1000 mm/s. The tool velocity should be minimized to a reasonable level to avoid negative influence of artificial dynamic effect in explicit forming simulation. To explore the effects of different material models (isotropic hardening model and NSK Swift model) in springback prediction, two forming simulation runs of QP980 are done and all the numerical parameters are the same except the hardening model.

3.2 Springback calculation

In springback calculation stage, two control options in LS-Dyna can be used to eliminate rigid body motion. One method is to define constraints at three nodes (CTN) and the other is

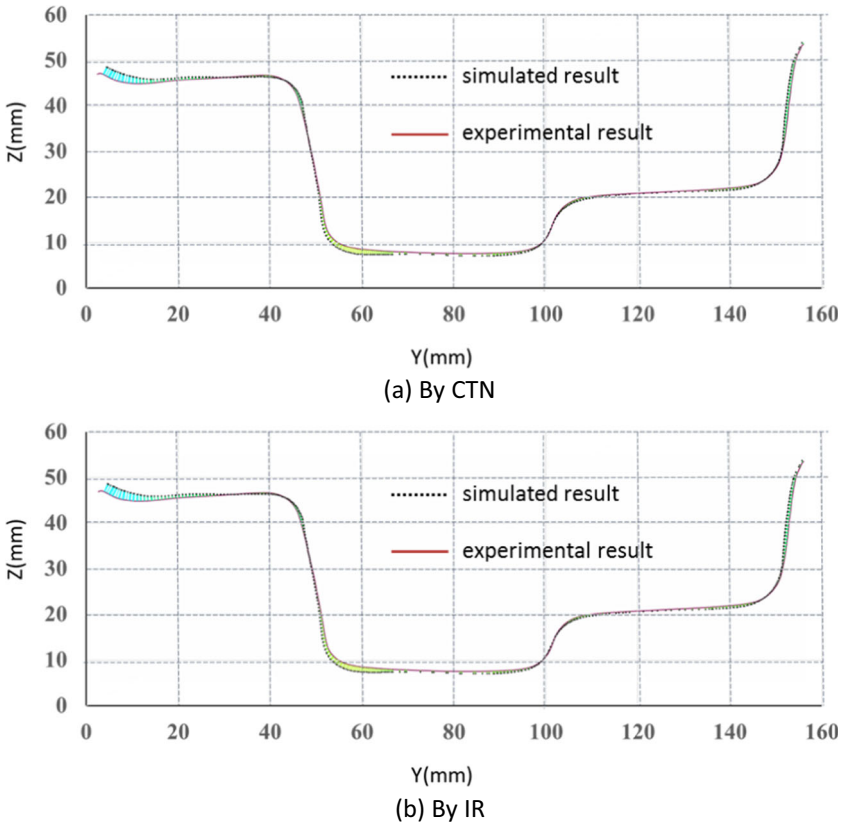

Fig. 8 Comparison between the experiment data and the simulated results of springback profiles at section II: **a** by CTN, **b** by IR

inertia relief (IR). As the springback experimental data is obtained without any boundary constraints, the inertia relief method which introduces no artificial deformation is selected to compute rigid body modes and then automatically constrain them out of the springback simulation. In this simulation, the THRESH value is set as the default value 0.02 Hz at first. It should be ensured that the threshold value is larger than the eigenvalues of the first six degrees which are available after calculation. Moreover, the double precision version solver of LS-Dyna shall be used to improve convergence in simulation.

To compare the accuracy and efficiency of the two control methods in springback, the method defining constraints is also adopted and each springback model using different control method is run with 20 CPUs and 6G memory on the same workstation.

The method to define constraints at nodes is given as Fig. 5, and the constrained locations are as follows: node a at (−250, 0, 15), node b at (237, −1, 15), and node c at (−250, −12, 15). Node a eliminates all translational modes while node b eliminates rotations about *y*- and *z*-axis node c eliminates rotation about *x*-axis.

4 Springback prediction results

4.1 Validation of inertia relief

The springback amount of numerical simulation and experiment data of QP980 provided by Baoshan Iron and Steel Co. Ltd. are compared by best fit alignment and deviation analysis. Three sections are specified for comparison: section I at $x = 0$ mm, section II at $x = -150$ mm ,and section III at $x = -360$ mm as shown in Fig. 6. The comparison results are shown in Figs. 7, 8, and 9.

It can be seen from Figs. 7, 8, and 9 that the numerical results of both the inertia relief approach and the constrained method achieve good agreement with the experiment data, confirming the accuracy of the inertia relief approach in springback calculation. Moreover, springback prediction by CTN is completed in 5.2 h, while the model using IR is completed in 3.07 h, and this shows that the IR method runs 40 % faster than the CTN method.

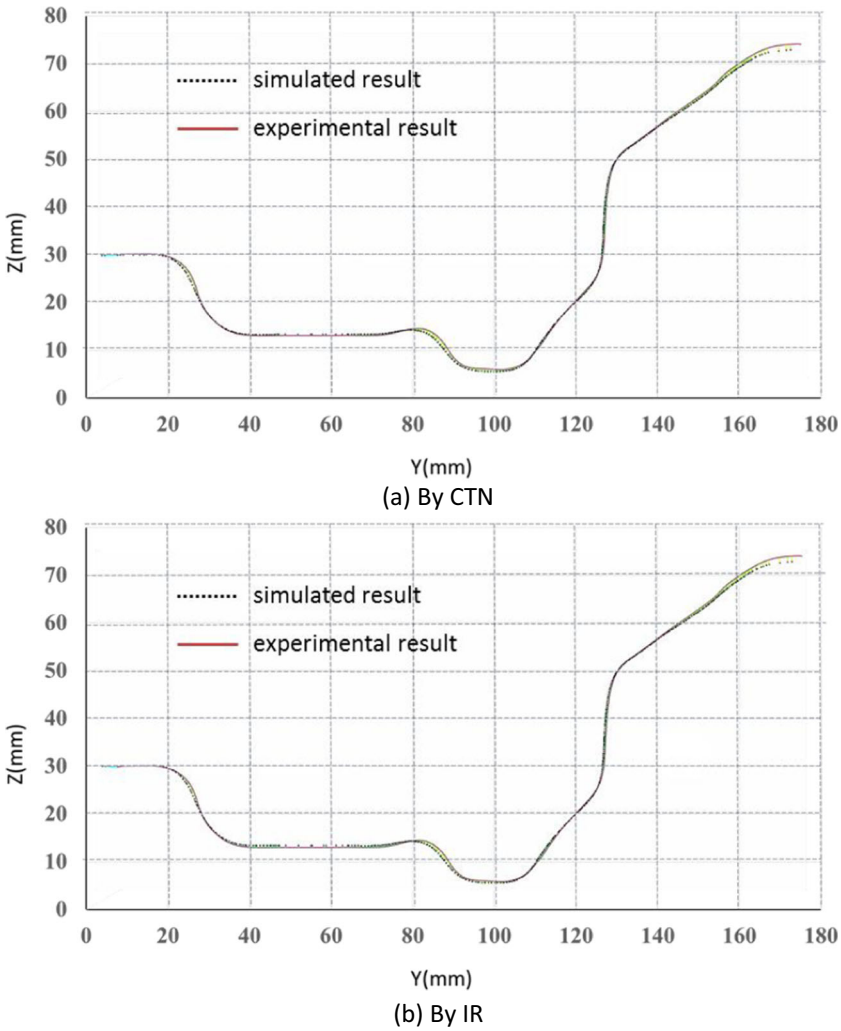

Fig. 9 Comparison between the experiment data and the simulated results of springback profiles at section III

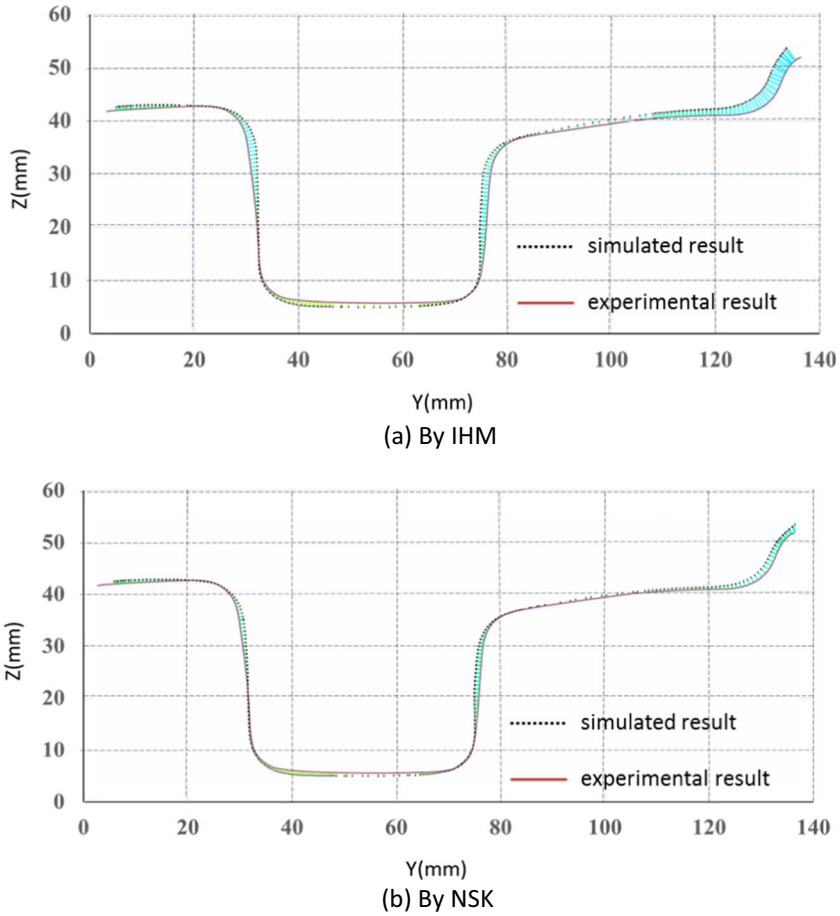

Fig. 10 Comparison between the experiment data and the simulated results of springback profiles at section I: **a** by IHM, **b** by NSK

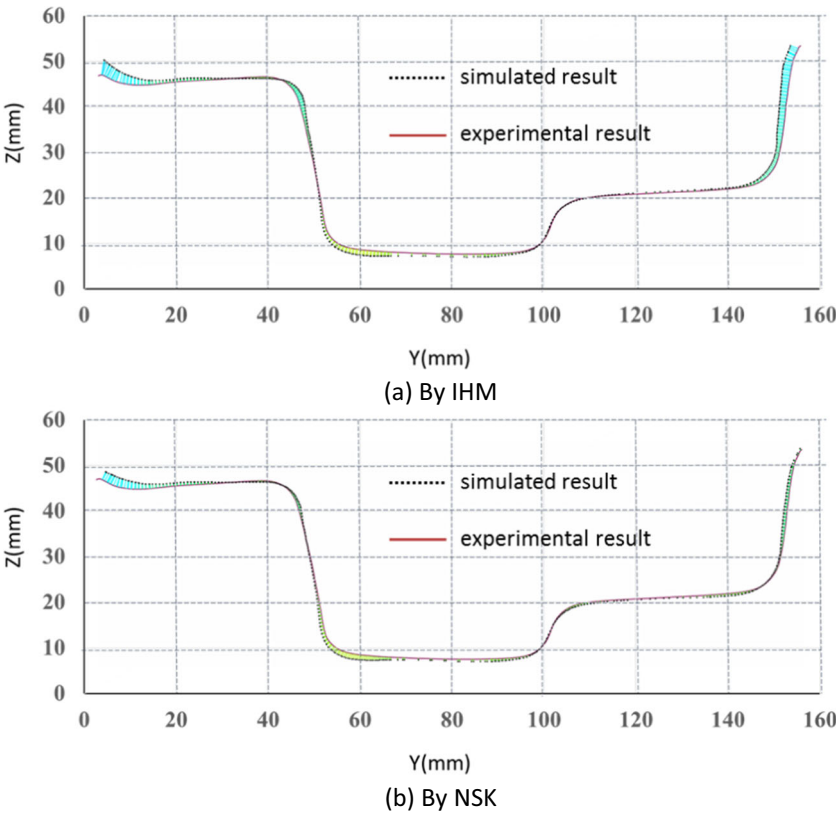

Fig. 11 Comparison between the experiment data and the simulated results of springback profiles at section II: **a** by IHM, **b** by NSK

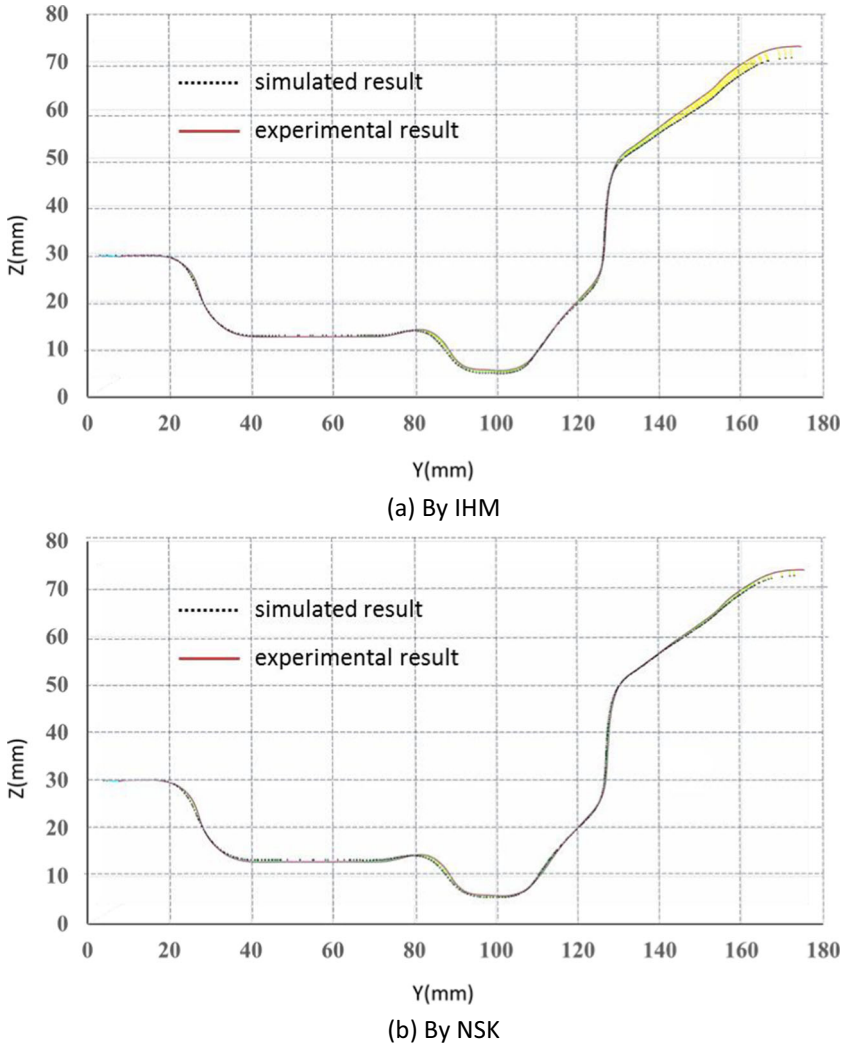

Fig. 12 Comparison between the experiment data and the simulated results of springback profiles at section III: **a** by IHM, **b** by NSK

4.2 Validation of the NSK Swift model

The numerical simulation results by using isotropic hardening model (IHM) and NSK kinematic hardening model and based on inertia relief are compared with the measured data of QP980 at three sections in Fig. 6. As shown in Figs. 10, 11, and 12, the solid line is the measured data and the dash line is the simulated springback profiles.

It can be seen from Figs. 10, 11, and 12 that the NSK Swift model gives nice springback prediction of QP980 compared with the experiment data. The average standard deviation values show that the NSK Swift model improves the springback prediction accuracy of QP980 greatly compared with that predicted by isotropic hardening model.

5 Springback compensation

The above work validates that NSK Swift model is much effective than isotropic hardening model in springback

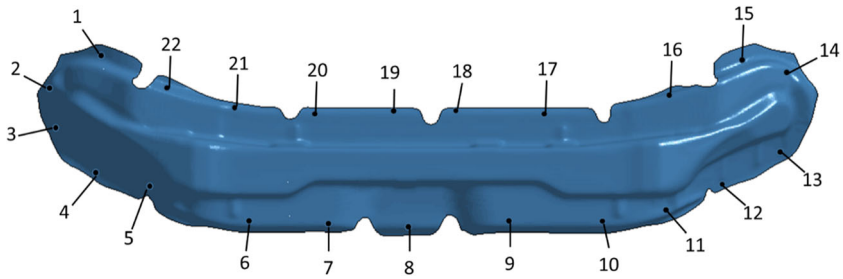

Fig. 13 The measuring points for shape deviation analysis

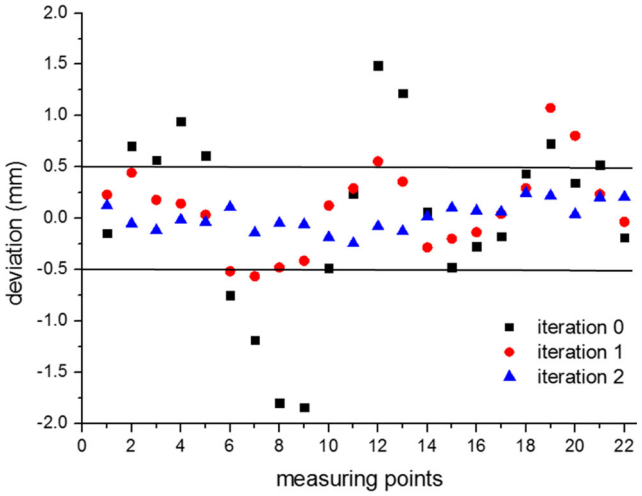

Fig. 14 Compensation results of different iteration on measuring points

prediction, so the NSK Swift model is employed in forming stage of the iterative compensation flow. As the NSK Swift model is not programmed with the solver for springback and compensation, the isotropic hardening model is still used in springback and compensation stage to improve calculation efficiency, which will not influence the accuracy as kinematic hardening does not occur in this two stages.

The setups for compensation with LS-Dyna are conducted as follows. The scale factor which decides the ratio of shape deviation in compensation is set as 0.7. The extrapolation algorithm for addendum and binder smooth is method 8, which can account for addendum and binder changes, and the smoothing level is set as 10. The options for undercut check and fix and tool element refinement are turned on. Noting that tools for the iterative compensation flow should be closed and the method defining real constrains is recommended for springback compensation.

To inspect the compensation results, the deviation between the springbacked part at different iterations and the design model are measured on 22 points as shown in Fig. 13.

As shown in Fig. 14, the shape deviation between the springbacked part and the designed model reaches the tolerance ±0.5 mm through two iterative compensations.

6 Conclusions

In the presented study, the NSK Swift model is proved to be able to well capture the kinematic hardening behaviors of QP9080 and the determining procedure of material constants of the NSK Swift model with tension data is relatively simple. Nice agreements between the measured data and the simulation result by the NSK Swift model have been achieved, which improves the springback prediction accuracy greatly compared with that predicted by isotropic hardening model.

As a new feature in LS-Dyna, the inertia relief approach is employed in springback calculation. The comparison of the two control methods shows that the inertia relief method is as accurate as the method to define constraints at nodes and improves the springback computational efficiency by 40 %. Moreover, the inertia relief approach does not need to define constrains on parts and introduces no artificial deformation, which better reflects the actual industrial production.

Based on the NSK Swift model, the springback compensation using LS-Dyna can reach acceptable tolerance through two iterations for this auto body penal.

It can be concluded that springback prediction of UHSS stamping with the NSK Swift model and inertia relief approach and springback compensation automatically with LS-Dyna are proved to be accurate and efficient, showing great significance in further industrial application.

It is worth comparing the NSK Swift model with other kinematic hardening models, such as Yoshida-Uemori model and Chaboche model in springback prediction of typical beam member components which have much larger springback, and distortional springback in some critical sections .

Acknowledgments The authors would like to thank Baoshan Iron and Steel Co. Ltd. for funding this research and providing the experimental data, we are grateful for the sincere support provided by Dr. Xinhai Zhu and Dr. Yuzhong Xiao from LSTC in using the new functionalities of LS-Dyna.

References

1. Ding L, Lin JP, Pang Z (2013) Experimental study on the forming limit diagram of QP980 under variable pressing velocities. Appl Mech Mater 275:1870–1873
2. Xie H, Dong X, Wang Q, Peng F, Liu K, Wang X, Wang J (2016) Investigation on transient electrically-assisted stress relaxation of QP980 advanced high strength steel. Mech Mater 93:238–245
3. Gao XL, Min JY, Zhang L, Li QC, Lian CW, Lin JP (2016) Prediction and experimental validation of forming limit curve of a quenched and partitioned steel. J Iron Steel Res Int 23(6):580–585
4. Wagoner RH, Lim H, Lee MG (2013) Advanced issues in springback. Int J Plasticity 45:3–20
5. Zeng D, Xia ZC (2005) An anisotropic hardening model for springback prediction. AIP Conf Proc. Institute of physics publishing LTD 778(A):241–246
6. Marretta L, Di Lorenzo R (2010) Influence of material properties variability on springback and thinning in sheet stamping processes: a stochastic analysis. Int J Adv Manuf Tech 51(1–4):117–134
7. Hill R (1950) The mathematical theory of plasticity. Oxford University Press, Oxford
8. Hill R (1948) Theory of yielding and plastic flow of anisotropic metals. Proc Roy Soc A 193:281–297
9. Barlat F, Lian K (1989) Plastic behavior and stretchability of sheet metals. Part I: a yield function for orthotropic sheets under plane stress conditions. Int J Plasticity 5(1):51–66
10. Armstrong PJ, Frederick CO (1966) A mathematical representation of the multiaxial Bauschinger effect. Central Electricity Generating Board [and] Berkeley Nuclear Laboratories, Research & Development Department

11. Chaboche JL, Jung O (1997) Application of a kinematic hardening viscoplasticity model with thresholds to the residual stress relaxation. Int J Plasticity 13(10):785–807
12. Chun BK, Jinn JT, Lee JK (2002) Modeling the Bauschinger effect for sheet metals, part I: theory. Int J Plasticity 18(5):571–595
13. Yoshida F, Uemori T (2002) A model of large-strain cyclic plasticity describing the Bauschinger effect and workhardening stagnation. Int J Plasticity 18(5):661–686
14. Eggertsen PA, Mattiasson K (2010) On constitutive modeling for springback analysis. Int J Mech Sci 52(6):804–818
15. Xiao Y, Chen J, Cao J (2012) A generalized thermodynamic approach for modeling nonlinear hardening behaviors. Int J Plasticity 38:102–122
16. Chen J, Xiao Y, Ding W, Zhu X (2015) Describing the non-saturating cyclic hardening behavior with a newly developed kinematic hardening model and its application in springback prediction of DP sheet metals. J Mater Process Tec 215:151–158
17. Liao L (2011) A study of inertia relief analysis. Proceedings of the 52nd AIAA/ASCE/AHS/ASC Structures, Structural Dynamics and Materials Conference. AIAA, Denver, CO, pp. 1–10
18. Nelson MF, Wolf JA (1977) The use of inertia relief to estimate impact loads. SAE Technical Paper: No. 770604
19. Baskar S (1998) Door structural slam durability inertia relief approach. SAE Technical Paper: No. 982309
20. Anvari M, Beigi B (1999) Automotive body fatigue analysis—inertia relief or transient dynamics?. SAE Technical Paper: No. 1999–01-3149
21. Singh M (2013) Life prediction of a refuse truck cab for automatic side loading operation using inertia relief. SAE Technical Paper: No. 2013–01-2011
22. Wagoner RH (2002) Fundamental aspects of springback in sheet metal forming. Proceedings NUMISHEET 2002:13–19
23. Wagoner RH, Gan W, Mao K, Price S, Rasouli F (2003) Design of sheet forming dies for springback compensation. Proceedings of the 6th International ESAFORM Conference
24. Weiher J, Rietman B, Kose K, Ohnimus S, Petzoldt M (2004) Controlling springback with compensation strategies. AIP confer proc American Institute of Physics 712:1011–1015
25. Lingbeek R, Huetink J, Ohnimus S, Petzoldt M, Weiher J (2005) The development of a finite elements based springback compensation tool for sheet metal products. J Mater Process Tec 169(1):115–125
26. Yang XA, Ruan F (2011) A die design method for springback compensation based on displacement adjustment. Int J Mech Sci 53(5):399–406
27. Li G, Liu Y, Du T, Tong H (2014) Algorithm research and system development on geometrical springback compensation system for advanced high-strength steel parts. Int J of Adv Manuf Tech 70(1–4):413–427
28. Dan J, Lancheng W (2006) Direct generation of die surfaces from measured data points based on springback compensation. Int J of Adv Manuf Tech 31(5–6):574–579
29. Wang H, Zhou J, Zhao T, Tao Y (2015) Springback compensation of automotive panel based on three-dimensional scanning and reverse engineering. Int J Adv Manuf Tech:1–7. doi:10.1007/s00170-015-8042-x
30. Wang H, Zhou J, Zhao TS, Liu LZ, Liang Q (2016) Multiple-iteration springback compensation of tailor welded blanks during stamping forming process. Mater Design 102:247–254
31. Xiao Y, Chen J, Zhu X, Cao J (2013) Modified maximum mechanical dissipation principle for rate-independent metal plasticity. J Appl Mech-T ASME 80(6):061020
32. Pagaldipti N, Shyy YK (2004) Influence of inertia relief on optimal designs. Proceedings of the 10th AIAA/ISSMO multidisciplinary analysis and optimization conference. American Institute of Aeronautics and Astronautics (AIAA) 1:616–621